

Tight-binding-based empirical potentials: molecular dynamics of wafer bonding

Kurt Scheerschmidt*, Detlef Conrad, YuChen Wang

Max Planck Institute of Microstructure Physics, Weinberg 2, D-06120 Halle/Saale, Germany

Accepted 2 April 2001

7 Abstract

8 Molecular dynamics simulations using tight-binding methods or based on an empirical potential derived from the
9 tight-binding approximation have been employed to describe atomic interactions at interface created by the macro-
10 scopic wafer bonding process. The bond order potentials including π -bonds are used to predict the interaction of di-
11 amond wafer surfaces: strong covalent bonding is possible for flat and clean C(001)-2 × 1 surfaces under ultrahigh
12 vacuum (UHV) conditions and at room temperature, C(111)-2 × 1 surfaces will bond very weakly and debond already
13 at moderate temperatures. © 2001 Elsevier Science B.V. All rights reserved.

15 1. Introduction

16 Wafer bonding, i.e. the creation of interfaces by
17 joining two wafer surfaces, has become an attrac-
18 tive method for many practical applications to
19 microelectronics, micromechanics or optoelec-
20 tronics [1]. For biomedical applications it is de-
21 sirable to bond together diamond layers with no
22 intermediate bonding layer present. Silicon–silicon
23 bonding is possible without an intermediate
24 bonding layer if performed under ultrahigh vac-
25 uum (UHV) conditions. Covalent bonding of sili-
26 con can thus be accomplished even at room
27 temperature as also predicted by molecular dy-
28 namics simulations [2,3]. Subsequently, UHV
29 bonding of GaAs/GaAs and InP/GaAs has also
30 been shown to work successfully [4,5].

31 However, the atomic processes determine the
32 behavior of extended defects at a microscopic le-
33 vel, thus influencing the macroscopic properties of
34 bonded materials. While, in principle, it is now
35 possible to predict material properties by using
36 quantum-theoretical ab initio calculations with a
37 minimum of free parameters, the only method to
38 simulate atomic processes with macroscopic rele-
39 vance is the molecular dynamics (MD) method
40 using suitably fitted many-body empirical poten-
41 tials. Investigating perfect or distorted surfaces
42 (steps, reconstruction, adsorbates, facets, mistilt,
43 twist rotation) of different semiconductor materi-
44 als enables one to study the elementary processes
45 and the resulting defects at the interfaces as well as
46 to characterize the ability of the potentials itself.

47 The MD simulations have successfully been
48 used to describe UHV bonding experiments for
49 Si(100) [3], and hydrogen-passivated hydrophobic
50 bonding process [6], and to analyze the defect
51 structure at bonded interfaces [7–9]. For instance,
52 starting with two perfect and parallel-oriented Si

* Corresponding author. Tel.: +49-345-558-2910; fax: +49-345-558-2917.

E-mail address: schee@mpi-halle.de (K. Scheerschmidt).

53 blocks with perfectly aligned 2×1 reconstructed
54 (1 0 0) surfaces yields perfectly bonded structures.
55 Fast heat transfer, 90° starting configuration, or
56 including steps or small rotational misorientations
57 result in configurations no longer perfectly coordi-
58 nated. After bonding over steps partial disloca-
59 tions are left or special structural units occur,
60 called the 42m dreidel. The screw dislocations
61 forming the network of the (0 0 1) low-angle twist
62 grain boundary can dissociate intrinsically into
63 two 30° partials along the $\{1\ 1\ 1\}$ glide planes, and
64 the nodes at the intersections are formed by sym-
65 metrical characteristic groups of atoms. Little has
66 been reported on the bonding of amorphous silica
67 (α -SiO₂) surfaces [10,11], which may be the basis
68 to describing hydrophilic wafer bonding. In addi-
69 tion, the transferability of the simulations to other
70 materials systems is not well suited up to now. On
71 the other hand, conventional transmission (TEM)
72 and high-resolution electron microscopy (HREM)
73 structure imaging has been applied to investigate
74 the resulting interfaces and the defect structures at
75 an atomic level [12], which in combination with
76 calculated IR spectra provides a good experimen-
77 tal evidence of the results.

78 As in the case of silicon wafer bonding, MD
79 simulations are applied to understand the atomic
80 processes at the interfaces of bonded diamond
81 structures. Special attention will be drawn to the
82 question of whether the energy locally released
83 during the bonding process may lead to the
84 transformation of thermodynamically metastable
85 diamond to thermodynamically stable graphite.
86 Such a graphitization process prevents the use of
87 bonded diamond layers in devices because of the
88 poor mechanical properties of graphite layers.

89 2. Method

90 The modeling of the interaction of diamond
91 surfaces by molecular dynamics simulations is far
92 more difficult than for silicon as the π -bonding
93 character at the surfaces has to be considered.
94 Calculations based on a full quantum mechanical
95 description are far too time-consuming for ma-
96 croscopically relevant systems. Simple models
97 based, for instance, on the Stillinger–Weber po-

tential or the Tersoff potential (which were used 98
successfully for silicon [3–9]) are inappropriate to 99
describe the properties of different carbon struc- 100
tures. In particular, a model that will predict reli- 101
ably how diamond surfaces interact must at least 102
describe diamond, graphite and the diamond sur- 103
faces correctly. 104

Therefore, it is of importance to find physically 105
motivated semi-empirical potentials starting 106
mostly with the moments of the electron density 107
and using tight-binding representations [13]. A 108
second moment approximation of the tight-bind- 109
ing model can be used to establish a general form 110
at the level of the Tersoff potential with at least 111
only four free fit parameters [14,15]. A further 112
enhancement is possible based on the bond order 113
potential (BOP4) [16,17], which is given up to the 114
further-level continued fraction of the Greens 115
function. Its ability is demonstrated in the fol- 116
lowing (see also [18,19]); the details will be pub- 117
lished elsewhere. Fig. 1 describes schematically the 118
relation between the bond order terms used in the 119
Tersoff potential and the steps in the derivation of 120
the analytical form of the bond order potentials. 121
We use an orthogonal tight-binding model in the 122
parametrization of Xu et al. [20] to describe the 123
interatomic interactions. The molecular dynamics 124
simulations are performed using the implementa- 125
tion of Horsfield et al. [17]. Within this model, the 126
exact tight-binding bond orders are approximated 127
by analytical expressions for the σ - and the π - 128
bond, hence allowing molecular dynamics simu- 129
lations at a speed comparable to that achieved by 130
other empirical methods. Since the bond orders 131
predicted by this model are in good agreement 132
with the exact bond orders, the simulations of free 133
surfaces and interacting surfaces agree well with 134
the tight-binding results as shown in the results 135
below. The model is able to describe carbon in the 136
graphitic and diamond phases reasonably well. 137
The bond lengths and energies of the C(0 0 1)- 2×1 138
and the C(1 1 1)- 2×1 reconstruction are in good 139
agreement with the experimental results and 140
quantum mechanical calculations. 141

Tersoff and BOP potentials

Tersoff: empirical *bond order* potential

$$V \sim \sum [\exp(-\lambda r_{ij}) - b_{ij} \exp(-\mu r_{ij})]$$

bonds are weighted by $b_{ij} \sim F(r_{ik}, r_{jk}, \gamma_{ijk})$
over all neighbours k and with all parameters fitted

BOP: bond order approximation justified by TB methods

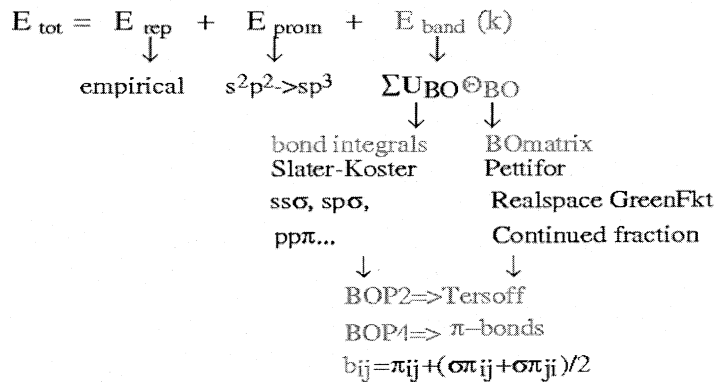


Fig. 1. Bond order terms used in the Tersoff potential versus the derivation of the analytical form of the bond order potentials.

142 **3. Results**

143 The simulations show that covalent bonds can
 144 form between C(001)-2 × 1 surfaces already at
 145 room temperature. Fig. 2(a) shows the result of the
 146 simulation for a small cell using a tight-binding
 147 MD. The tight-binding level of the simulation is
 148 necessary to describe π -bonds correctly. Both di-
 149 rect tight-binding and the semi-empirical MD using
 150 a BOP4 potential, which, however, enables one
 151 to use far more atoms in the calculation, show the
 152 same bonding behavior, i.e. structures and energies.
 153 The dimerized structure of the surfaces are
 154 still present but the bonds change from the “double
 155 bond” character to a “single bond” one, with
 156 an interface of fourfold coordinated atoms forming.
 157 Due to the broken π -bond of the dimer, the
 158 dimer bond length increase from 1.4 to 1.67 Å, the
 159 bond length between the dimers of the two sur-
 160 faces is 1.55 Å and the interface energy is
 161 6.57 J/m². For a 90° twist rotation or monoatomic
 162 steps, covalent bonding is possible, too, leading to

163 the dreidel structure as in silicon [7] and an energy
 164 of 6.72 J/m².

165 Using a similar starting configuration for
 166 C(111)-2 × 1 surfaces, the simulations show that
 167 the surfaces repel each other rather than form a
 168 covalently bonded interface because the environ-
 169 ment of the surface atoms is far more graphite-like
 170 than that of the C(001)-2 × 1 surfaces, preventing
 171 spontaneous bonding. However, covalent bonding
 172 can be achieved if one starts with a distance be-
 173 tween the surfaces of about 1.8 Å, which might be
 174 realized via weak external forces or van der Waals
 175 forces. In this case, small structural changes (i.e.
 176 bond lengths and bond angles) within the surfaces
 177 allow the bonding between them, as shown in Fig.
 178 2(b), here applying the BOP4 potential. There is
 179 almost no energy gain from such an interface
 180 compared to two isolated surfaces. Simulations at
 181 room temperature show that the surfaces stick
 182 together indicating that there is an energy barrier
 183 to separate them again. At a simulation tempera-
 184 ture of approximately 500 K the surfaces debond.

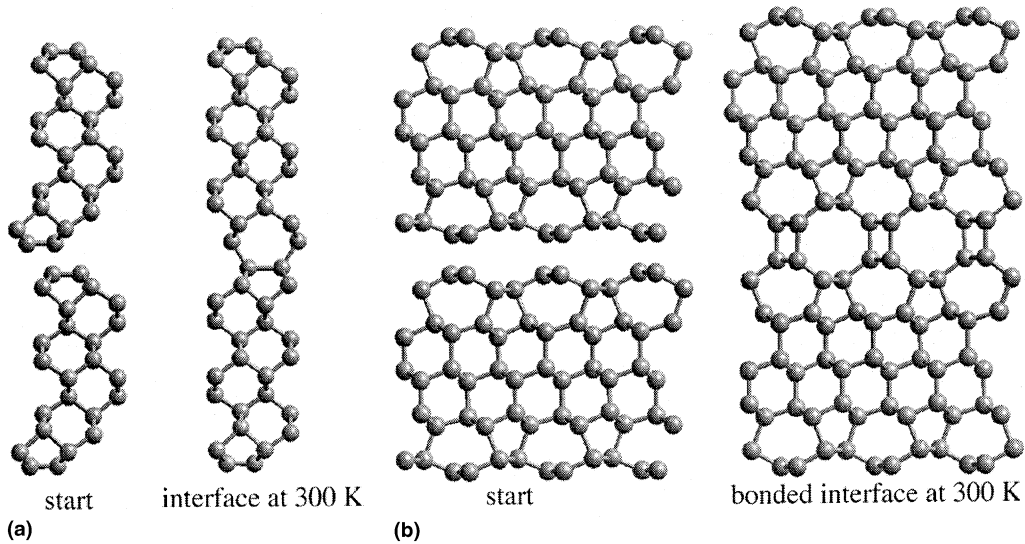


Fig. 2. MD simulations of bonding diamond surfaces: (a) C(001)-2 × 1 with tight-binding MD, (b) C(111)-2 × 1 and using a BOP4 potential.

185 For room temperature bonding, the simulations
 186 predict no graphitization. While the interface
 187 consisting of C(111) surfaces debonds already at
 188 moderate temperatures, the interfaces generated of
 189 C(001) surfaces are predicted to be very stable.
 190 Graphitization along the (111) planes occurred at
 191 approximately 2000 K. It turned out to be im-
 192 possible to create a perfect bulk material by heat-
 193 ing up the interface and breaking the dimer bonds.
 194 This is demonstrated in Fig. 3, showing typical

195 examples of incomplete bonding at C(111) sur-
 196 faces. Because of the weak bonding of the C(111)
 197 surfaces, debonding occurs at steps as shown both
 198 for the mono- and the diatomic step structures in
 199 Figs. 3(a) and (b), respectively. Fast heat transfer
 200 results in metastable configurations fivefold bon-
 201 ded as in Fig. 3(c). The metastable configurations
 202 may be generated due to restriction of the next
 203 neighbor interaction of the short-range BOP po-
 204 tential. To overcome this deficiency the interlayer

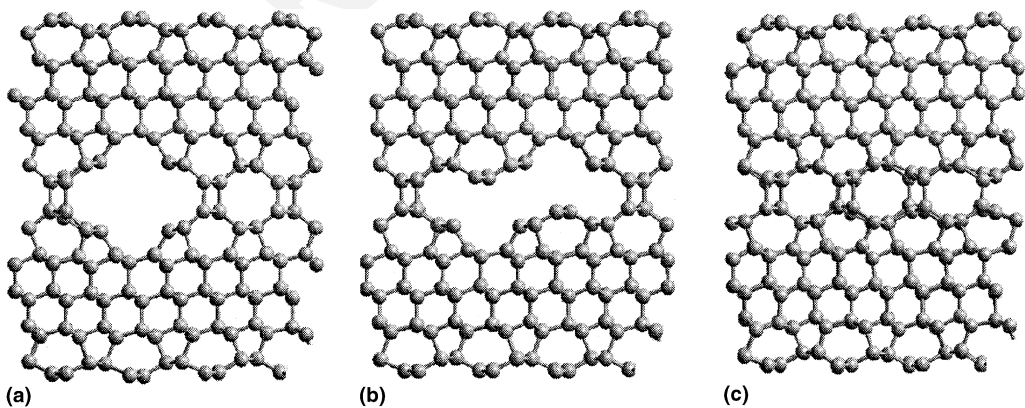


Fig. 3. MD simulations of metastable structures at bonded C(111)-2 × 1 surfaces: (a) interacting monoatomic steps, (b) debonding at diatomic steps, and (c) fivefold bonds as result of fast heat transfer.

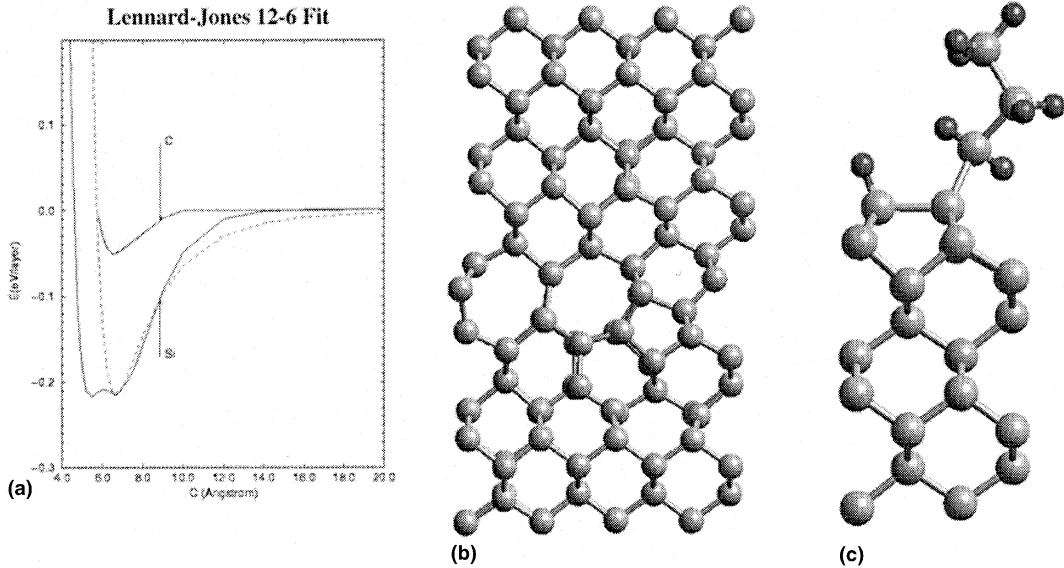


Fig. 4. (a) The interaction minimum energy for graphite C and “graphitic” Si as function of the lattice parameter c (continuous curves, DFT database with optimized lattice constants $a_C = 0.244$ nm and $a_{Si} = 0.386$ nm) and for best Lennard–Jones fit (dashed curves), (b) C(001)- 2×1 bonding over steps, and (c) C₃H₇ radical attached to a C(001)- 2×1 :H surface (one H is desorbed and not shown).

205 forces must be included into the empirical poten-
 206 tial by combining smoothly a suitably paramet-
 207 rized short-range potential with a long-range
 208 potential at a common cutoff. Fig. 4(a) shows the
 209 fit of a Lennard–Jones potential to a LDA data
 210 basis varying the c/a ratio of the lattice constants
 211 up to the minimum which characterizes the phys-
 212 ical absorption [21].

213 The effect of surface steps is of great interest
 214 because it is important to know whether surfaces
 215 steps will prevent the formation of a continuous
 216 interface, or whether bonding over steps is possible
 217 as in the case of silicon. For simulations including
 218 surface steps, much bigger models are necessary,
 219 which can be described solely using the BOP4
 220 potential. To investigate the effect of surface steps,
 221 we prepared a model in which both of the inter-
 222 acting surfaces had a monoatomic height step. At
 223 room temperature, the upper terraces interact as in
 224 the case of perfect surfaces. The lower terraces are
 225 too far apart so that no bonds form between them.
 226 The simulation shows, however, that bonding over
 227 steps is possible at elevated temperature without
 228 melting the bulk material or transformation to
 229 graphite (Fig. 4(b)).

Inspired by most recent experiments [22] we 230
 have also investigated how passivated surfaces can 231
 be bonded via reactive organic molecules. In the 232
 experiments, complex long-chained organic mole- 233
 cules with reactive end-groups are used. Our tight- 234
 binding simulations predict that hydrocarbon 235
 radicals can be attached to a hydrogen-passivated 236
 C(001)- 2×1 surface, see Fig. 4(c). Wafer bonding 237
 will then be possible if a similar reaction occurs on 238
 a second surface. 239

4. Conclusion 240

The simulations show that covalent bonding of 241
 diamond surfaces should be possible provided the 242
 surfaces are sufficiently flat. Polycrystalline wafers, 243
 C(111) wafers or silicon covered with a diamond- 244
 like carbon layer, where a more graphite-like envi- 245
 ronment of the surface atoms is expected, are 246
 probably far more difficult to bond covalently than 247
 are C(001) or silicon surfaces. Bonding over steps 248
 will be possible only at elevated temperatures. 249
 Hydrogen-passivated surfaces are likely to bond 250
 via reactive organic molecules. Thus, simulations 251

252 based on potentials derived from the bond order
 253 expansion are used to enhance the physical reli-
 254 ability of the method and to predict the bonding
 255 behavior of a wide variety of semiconductors.

256 **References**

257 [1] Q.Y. Tong, U. Gösele, *Semiconductor Wafer Bonding:*
 258 *Science and Technology*, Wiley, New York, 1999.
 259 [2] U. Gösele, H. Stenzel, T. Martini, J. Steinkirchner, D.
 260 Conrad, K. Scheerschmidt, *Appl. Phys. Lett.* 67 (1995)
 261 3614.
 262 [3] D. Conrad, K. Scheerschmidt, U. Gösele, *Appl. Phys. A* 62
 263 (1996) 7.
 264 [4] T. Akatsu, A. Plöbl, H. Stenzel, U. Gösele, in: 5th
 265 International Symposium on Semiconductor Wafer Bond-
 266 ing, Proceedings of the Electrochemical Society, Penning-
 267 ton, NJ, 1999, in press.
 268 [5] T. Akatsu, A. Plöbl, H. Stenzel, U. Gösele, *J. Appl. Phys.*
 269 86 (1999) 7146.
 270 [6] D. Conrad, K. Scheerschmidt, U. Gösele, *Appl. Phys. Lett.*
 271 71 (1997) 2307.
 272 [7] A.Y. Belov, D. Conrad, K. Scheerschmidt, U. Gösele,
 273 *Philos. Mag. A* 77 (1998) 55.

[8] A.Y. Belov, K. Scheerschmidt, U. Gösele, *Phys. Status Solidi A* 171 (1999) 159. 274
 275
 [9] A.Y. Belov, R. Scholz, K. Scheerschmidt, *Philos. Mag.* 276
 Lett. 79 (1999) 531. 277
 [10] S.H. Garofalini, *Electrochem. Soc. Proc.* 93-29 (1994) 57. 278
 [11] D. Timpel, M. Schaible, K. Scheerschmidt, *J. Appl. Phys.* 279
 85 (1999) 2627. 280
 [12] K. Scheerschmidt, D. Conrad, A. Belov, H. Stenzel, 281
Electrochem. Soc. Proc. 97-36 (1998) 381. 282
 [13] C.M. Goringe, D.R. Bowler, E. Hernandez, *Rep. Prog. Phys.* 60 (1997) 1447. 283
 284
 [14] D. Conrad, K. Scheerschmidt, *Phys. Rev. B* 58 (1998) 4538. 285
 [15] D.G. Pettifor, *Phys. Rev. B* 63 (1989) 2480. 286
 [16] D.G. Pettifor, I.I. Oleinik, *Phys. Rev. B* 59 (1999) 8487. 287
 [17] A.M. Horsfield, A.M. Bratkovski, M. Fearn, D.G. Pettifor, M. Aoki, *Phys. Rev. B* 53 (1996) 12694. 288
 289
 [18] K. Scheerschmidt, D. Conrad, A. Belov, D. Timple, *Mater. Sci. Semicond. Proc.* 3 (2000) 129. 290
 291
 [19] D. Conrad, K. Scheerschmidt, U. Gösele, *Appl. Phys. Lett.* 292
 77 (2000) 49. 293
 [20] C.H. Xu, C.Z. Wang, C.T. Chan, K.M. Ho, *J. Phys. Condens. Matter* 4 (1992) 6047. 294
 295
 [21] Y.C. Wang, K. Scheerschmidt, U. Gösele, *Phys. Rev. B* 61 (2000) 12864. 296
 297
 [22] A. Plöbl, G. Kräuter, *Mater. Sci. Eng. R* 25 (1999) 1. 298